The FT absorption spectrum of 13CH12CH (III): vibrational states in the range 6750 to 9500 cm-1.

Gianfranco Di Lonardo, Luciano Fusina, Filippo Tamassia, André Fayt, Séverine Robert, Jean Vander Auwera, Michel Herman

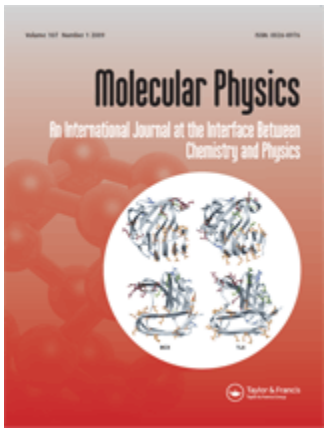

The FT absorption spectrum of $^{13}CH^{12}CH$ (III): vibrational states in the range 6750 to 9500 cm^{-1}.

Journal:	*Molecular Physics*
Manuscript ID:	TMPH-2008-0023.R1
Manuscript Type:	Full Paper
Date Submitted by the Author:	22-Feb-2008
Complete List of Authors:	di Lonardo, Gianfranco; Università di Bologna, Dipartimento di Chimica Fisica e Inorganica Fusina, Luciano; Università di Bologna, Dipartimento di Chimica Fisica e Inorganica Tamassia, Filippo; Università di Bologna, Dipartimento di Chimica Fisica e Inorganica Fayt, André; Université Catholique de Louvain Robert, Séverine; Université Libre de Bruxelles Vander Auwera, Jean; Université libre de Bruxelles, Chimie quantique et Photophysique Herman, Michel; Université Libre de Bruxelles, Chimie quantique et Photophysique
Keywords:	13CH12CH, Infrared Fouruer transform, vibrational spectroscopy, overtones, acetylene

Molecular Physics
12 July 2010

The FT absorption spectrum of $^{13}CH^{12}CH$ (III): vibrational states in the range 6750 to 9500 cm^{-1}

G. Di Lonardo[1], L. Fusina[1], F. Tamassia[1],A. Fayt[2], S. Robert[3*], J. Vander Auwera[3], and M. Herman[3]**

[1] Dipartimento di Chimica Fisica e Inorganica
Università di Bologna
Viale Risorgimento, 4
I-40136, Bologna
Italy

[2] Laboratoire de Spectroscopie Moléculaire
Université Catholique de Louvain
Chemin du Cyclotron, 2
B-1348 Louvain-La-Neuve
Belgium

[3] Service de Chimie quantique et Photophysique CP160/09
Université Libre de Bruxelles (U.L.B.)
Av. Roosevelt, 50
B-1050, Bruxelles
Belgium

* F.R.I.A. researcher
**Senior Research Associate with the Fonds National de la Recherche Scientifique (Belgium)

Pages: 14
Figures: 4
Tables: 1

Send mail to Prof. Di Lonardo
Email : dilo@ms.fci.unibo.it

Abstract

Forty cold bands and 29 hot bands are reported from the high resolution FT absorption spectrum of $^{13}CH^{12}CH$, all leading to vibrational states located between 6750 and 9500 cm^{-1}. Each of these bands has been vibrationally assigned and rotationally analysed. The band centres (ν_c), vibrational term values (G_v) and rotational constants are listed.

1. Introduction

This work is the next contribution of the Bologna-Louvain-Brussels collaboration to the systematic investigation of the mid and near infrared absorption spectrum of $^{13}CH^{12}CH$ using high resolution Fourier transform spectroscopy (FTS). The ranges 3800-6750 [1] and 9500-10000 [2] cm^{-1} were considered in two previous, recent papers. Even earlier studies focused either on the lower energy region [3-5], or on overtones recorded using Fourier transform intracavity laser absorption spectroscopy [6]. The present investigation fills the remaining energy gap, thus between 6750 and 9500 cm^{-1}. The spectrum in this range is quite dense and shows numerous perturbation features whose assignment required significant advances in the global analysis of $^{13}CH^{12}CH$. Initial attempts along this line first considered only the vibrational degrees of freedom [7], soon followed by decisive results on the vibration-rotation global analysis [8]. The latter investigation successfully accounted in a single process for all 12703 vibration-rotation lines reported in the literature that involved energy levels up 6750 cm^{-1}. The resulting rotational constants and polyad matrix model were used in the present investigation to predict vibration-rotation energy states above 6750 cm^{-1}, which ~~significantly~~ helped in the assignment process. The inclusion in the global procedure of the presently assigned lines will require intensive additional work, not finalized at this stage of the investigation.

The usual vibrational numbering in acetylene is used throughout the paper, namely ν_1 and ν_3 for the symmetric (σ^+) and antisymmetric (σ^+) CH stretchings, respectively, ν_2 for the CC stretching (σ^+), and ν_4 and ν_5 for the degenerate *trans* (π) and *cis* (π) bendings, respectively. The vibrational quantum numbers l_4 and l_5, with $k = l_4+l_5$ are used with the same sign convention as in the recent papers in the present series, thus

different from the one used in the previous reports on acetylene from the Bologna and Brussels groups, to agree with the one defined in the global analysis computer package developed in Louvain [9,10].

2. Experimental

The spectra are the same as those reported in [1] and the reader is referred to that paper for all experimental details. An isotopically enriched sample of $^{13}CH^{12}CH$ synthesised with an isotopic purity close to 99% was used and the spectra were recorded at ULB using a Bruker IFS120HR Fourier transform spectrometer.

Seven spectra were recorded at a resolution of 0.01 cm^{-1} (maximum optical path difference of 90 cm), sample pressures ranging between 0.037 and 48.40 hPa and an absorption path length of 55.1 m. The studied regions were calibrated against transition wavenumbers of H_2O [11-12]. The resulting accuracy is better than 0.0005 cm^{-1} for strong isolated lines.

3. Vibrational structure

The vibrational structure in acetylene electronic ground state can be modelled using polyads or so-called vibrational clusters. These polyads are defined using the $\{N_s,N_r,k\}$ set of numbers, with $N_s = v_1+v_2+v_3$, $N_r = 5v_1+3v_2+5v_3+v_4+v_5$ and $k=l_4+l_5$, as summarized in [13]. They include off-diagonal elements corresponding to the following anharmonic resonances: 3/245, 1/244, 1/255, 44/55, 11/33, 1/245, 3/244, 3/255 and 14/35 with *e.g. i/jkk* meaning interaction terms of the type $\Delta v_i = \pm 1, \Delta v_j = \mp 1, \Delta v_k = \mp 2$ and characterized by the interaction constant $K_{i/jkk}$. All interaction matrix elements are detailed in [8].

Sixty nine vibrational bands were identified in the studied spectral range, all fitting within the polyad model. They include bands arising from the ground vibrational state and hot bands starting from $v_4 = 1$ or $v_5 = 1$ excited bending states. They altogether involve 52 different upper vibrational states. This number of states only represents around 2% of all expected vibrational levels in this region, all k-values considered. It also represents some 13% of all the expected Σ and Π states. In fact, we observe more than 21% of the Σ and Π expected states between 6999 and 7970 cm^{-1} and around 8% of these same-symmetry states between 8414 and 9330 cm^{-1}. These bands are gathered in table 1. The wavenumbers listed in this table correspond to band centres and vibrational term values as resulting from the rotational analysis detailed in the next section. The states are assigned using the usual vibrational quantum numbers in acetylene, defined in the introduction. The assignments correspond, as usually, to the dominant zero order eigenvector in the corresponding polyad.

Preliminary results of the analysis of the spectral region presently considered were included in the global fit of Ref. [7]. A systematic investigation, which has never

been carried out previously, was undertaken to complete the study of the mid and near FTIR absorption spectrum of $^{13}CH^{12}CH$ up to 10000 cm^{-1}. Many more bands have been identified in the spectrum thanks to the detailed rotational analysis presently performed. The vibrational assignment was supported by the global vibration results recently published [7]. In very specific cases, predictions from the global fit were essential to the analysis. For instance, the *J*-numbering in the $3\nu_2+2\nu_4+3\nu_5 \leftarrow$GS ($\Pi$ - Σ^+) Q branch around 9029 cm^{-1} could not be reliably achieved from the conventional procedure and required the precise predictions from the global model. The present analysis led to modify a very limited number of previously published vibrational assignments, because the composition of the eigenvectors from the polyad matrix model changed very slightly.

The bands in the presently investigated spectral region are mainly grouped in three windows, centred at 6550, 7250 and 8500 cm^{-1}. In the low energy window the $\nu_1+\nu_3 \leftarrow$GS band (analysed in Ref. [1]) is the dominant feature. Medium intensity bands not reported before are $\nu_1+\nu_3+\nu_4 \leftarrow \nu_4$ and $\nu_1+\nu_3+\nu_5 \leftarrow \nu_5$. The 7250 cm^{-1} region is dominated by the Q-branches associated to the $\nu_1+\nu_3+\nu_4 \leftarrow$GS, $2\nu_3+\nu_5 \leftarrow$GS and $2\nu_1+\nu_5 \leftarrow$GS bands, with band centres at 7124.36, 7203.82 and 7393.02 cm^{-1}, respectively. In the highest energy window the strongest absorptions are given by $\nu_1+\nu_2+\nu_3 \leftarrow$GS and $3\nu_2+\nu_4+3\nu_5 \leftarrow$GS, centred at 8464.23 and 8475.69 cm^{-1}, respectively.

[Insert figure1 and 2 about here]

The richness of the spectra is illustrated in figures 1 to 4 that highlight selected ranges in the FT transmittance data. For instance, the role of anharmonic resonances in promoting the observation of zero order dark bands on the spectrum is evident in figures 1 and 2. In figure 1, the zero order dark band involving 7 quanta excitation ($2\nu_2+2\nu_4+3\nu_5$) is observed with an unusual intensity, if compared to that of the zero order bright band ($2\nu_3+\nu_5$). The intensity borrowing actually results from a complex interaction mechanism since there is no direct coupling between the two upper states. They, however, both belong to the same $\{N_s,N_r,k\}$ = {2,11,1} polyad and thus indirectly interact trough the ($\nu_2+\nu_3+\nu_4+2\nu_5$) dark state. The result of a more direct interaction within the {3,12,1} polyad is illustrated in figure 2. It involves the 1/255 anharmonic resonance connecting the upper states in the $\nu_1+2\nu_2+\nu_5$ and $3\nu_2+3\nu_5$ observed bands. The observation of all *k*-substates in the $2\nu_1+2\nu_5$ and $2\nu_1+\nu_4+\nu_5$ manifolds, through hot bands, is shown in figure 3. Eventually, the presence of the very weak $2\nu_1+\nu_4 \leftarrow$ GS band, that is forbidden by *u/g* selection rules in the main, symmetric isotopologue, is illustrated in figure 4. According to still preliminary extrapolations from the global model, the eigenvector analysis indicates that the composition of the upper Π level is as follows: $2\nu_1+\nu_4$ (77%), $\nu_1+\nu_3+\nu_5$ (15%), $2\nu_3+\nu_4$ (7%). Since all these zero order components lead to forbidden *g-g* transitions from the ground state in the main, symmetric isotopologue, none of them is expected to predominantly contribute to the intensity of the observed transition. It therefore must be due to symmetry-breaking within the normal mode picture.

[Insert figure 3 and 4 about here]

The origins of both the $1012^20(\Delta)\leftarrow\nu_4(\Pi)$ and $1012^00(\Sigma^+)\leftarrow\nu_4(\Pi)$ hot bands are predicted to fall roughly at 7104 cm^{-1}. Given the symmetry of the vibrational states involved, we expect $P_{e\leftarrow e}$, $Q_{e\leftarrow f}$ and $R_{e\leftarrow e}$ branches (where e and f are the conventional symmetry labels for the rotational levels) for the $\Sigma^+\leftarrow\Pi$ band and $P_{e\leftarrow e}$, $Q_{e\leftarrow f}$, $R_{e\leftarrow e}$, $P_{f\leftarrow f}$, $Q_{f\leftarrow e}$ and $R_{f\leftarrow f}$ branches for the $\Delta\leftarrow\Pi$ band. Three of these branches, namely $P_{e\leftarrow e}$, and $R_{e\leftarrow e}$ of the $\Sigma^+\leftarrow\Pi$ band and $Q_{e\leftarrow f}$ of the $\Delta\leftarrow\Pi$ band have not been observed at our level of sensitivity. This is somehow surprising, as we are confident that the predictions for the missing branches are rather accurate, since they involve the same upper rovibrational levels of the observed branches and, in addition, they are based on the spectroscopic parameters obtained from the corresponding cold bands, $1012^20(\Delta_e)\leftarrow$GS (Σ^+) and $1012^00(\Sigma^+)\leftarrow$GS (Σ^+) (centred at 7711.689 and 7711.692 cm^{-1}, respectively). At the moment we do not have a convincing explanation for that, except to call upon some unidentified perturbation, whose mechanism is not known, and which alters dramatically the intensity pattern. We believe that the inclusion of the presently reported bands in the rotation-vibration global fit will shed some light on this problem.

4. Rotational analysis

The rotational analysis of the bands listed in table 1 was performed using standard procedures. The energy of the rovibrational levels of the Σ^+ and Π states was calculated according to the expression:

$$T(v,J) = \tilde{\nu}_c + B_v J(J+1) - D_v \left[J(J+1)\right]^2 + H_v \left[J(J+1)\right]^3 \pm \tfrac{1}{2}\left\{q_v \left[J(J+1)\right] + q_v^J \left[J(J+1)\right]^2\right\} \quad (1)$$

with $\tilde{\nu}_c = G_v^{'} - B_v^{'}k^2 - G_v^{''} + B_v^{''}k^2$ and G_v the vibrational term value.

For the Δ state, the doubling of the rotational levels was modelled by:

$$\pm a\left\{\rho_v J(J+1) + \rho_v^J \left[J(J+1)\right]^2\right\}\left[J(J+1) - 2\right] \quad (2)$$

with a = ½ or ¼ for $(v_4^{l_4}, v_5^{l_5}) = (2^2, 0^0)$ and $(0^0, 2^2)$ or $(1^1, 1^1)$, respectively. In equations (1) and (2) upper signs refer to f–symmetry levels, lower signs to e–symmetry levels.

In addition, transitions whose wavenumbers differed from the corresponding calculated values by more than a chosen limit, ranging from 0.001 to 0.005 cm^{-1}, were excluded from the final cycle of the least-squares procedure.

The constants resulting from the band by band analysis procedure are listed in table 1. Although improved rotational constants resulted for the ground vibrational state from the global vibration-rotation analysis [8], we constrained them in the rotational analysis to the values in [3], to be consistent with the results in the neighbouring spectral ranges presented in the previous papers in the series [1,2]. The number of lines assigned in the branches and the number of fitted lines are indicated in table 1 for each band.

[Insert table 1 about here]

We decided to limit the number of fitted constants in the rotational analysis to the sextic term *H'*, as defined in equation (1). Actually, for many bands, additional terms in the *J*(*J*+1) expansion could as well be fitted and statistically determined. This behaviour

is typical whenever resonances occur, which are not accounted for in the band by band rotational model of equation (1). For the same reason, some of the distortion constants listed in table 1 are anomalously large or negative. One can notice that the same upper state is sometimes involved in both cold and hot bands. Upper state rotational constants usually slightly differ for these bands reaching the same upper state, because of the different number and measurement precision of the rotational lines included in the fitting procedure. All results will be merged when the global vibration-rotation fit will be extended to include the present spectral range.

Additional, weaker lines remain to be identified in the range presently studied. Some can tentatively be assigned to impurities in the sample, possibly $^{13}C^{12}CH_4$. Others probably arise from the studied species. Their rotational analysis and assignment need to be supported by the global vibration-rotation model that is being built simultaneously to the present investigation. They will be discussed at the final stage of the modelling process.

All line wavenumbers from the rotational analyses can be made available from the Bologna and Brussels authors.

6. Conclusions

We have reported on 69 absorption bands in $^{13}CH^{12}CH$ recorded using FTIR spectroscopy between the ranges of 2 and 3 CH excitation quanta, previously considered [1,2]. The 6750-9500 cm^{-1} range was not considered in previous studies devoted to detailed rotational analyses. Band origins and rotational constants were obtained from

band by band analysis. The present work thus completes the systematic vibration-rotation investigation of the FT absorption spectrum of the $^{13}CH^{12}CH$ molecule up to 1 μm, carried on in collaboration between Bologna, Brussels and Louvain-La-Neuve. Besides the current spectroscopic parameters of $^{13}CH^{12}CH$, the present study provides the information and assignments needed to expand the global vibration-rotation analysis up to higher energies, which will be attempted in the near future.

Acknowledgements

This work was sponsored, in Italy, by the Università di Bologna and MIUR (PRIN « Dinamiche molecolari ») and, in Belgium, by the Fonds National de la Recherche Scientifique (FNRS, contracts FRFC and IISN) and the « Action de Recherches Concertées de la Communauté française de Belgique ». It is performed within the "LEA HiRes " collaboration between ULB and UCL and was earlier supported by a bilateral scientific collaboration between the « Communauté française de Belgique » and FNRS (Belgium) and Italy.

References

[1] E. Cané, L. Fusina, F. Tamassia, A. Fayt, M. Herman, S. Robert, J. Vander Auwera, *Mol. Phys.* **104**, 515 (2006).

[2] G. Di Lonardo, L. Fusina, F. Tamassia, A. Fayt, S. Robert, J. Vander Auwera, M. Herman, *Mol. Phys.* **104**, 2617 (2006).

[3] G. Di Lonardo, A. Baldan, G. Bramati, L. Fusina, *J. Mol. Spectrosc.* **213**, 57 (2002).

[4] G. Di Lonardo, P. Ferracuti, L. Fusina, E. Venuti, J.W.C. Johns, *J. Mol. Spectrosc.* **161**, 466 (1993).

[5] L. Fusina, G. Bramati, A. Mazzavillani and G. Di Lonardo, *Mol. Phys*., **101**, 513 (2002).

[6] C. Depiesse, G. Di Lonardo, A. Fayt, L. Fusina, D. Hurtmans, S. Robert, F. Tamassia, J. Vander Auwera, A. Baldan, M. Herman, *J. Mol. Spectrosc.* **229**, 137 (2005).

[7] S. Robert, A. Fayt, G. Di Lonardo, L. Fusina, F. Tamassia, M. Herman, *J. Chem. Phys.* **123**, 174302/1 (2005).

[8] A. Fayt, S. Robert, G. Di Lonardo, L. Fusina, F. Tamassia, M. Herman, *J. Chem. Phys.* **126**, 114303/1 (2007).

[9] C. Vigouroux, A. Fayt, A. Guarnieri, A. Huckauf, H. Bürger, D. Lentz, D. Preugschat, *J. Mol. Spectrosc.* **202**, 1 (2000).

[10] A. Fayt, C. Vigouroux, F. Willaert, L. Margules, L.F. Constantin, J. Demaison, G. Pawelke, El Bachir Mkadmi, H. Bürger, *J. Mol. Struct.* **695-696**, 295 (2004).

[11] R.A. Toth, *Appl. Opt.* **32**, 7326 (1993).

[12] G. Guelachvili, K. Narahari Rao, *Handbook of Infrared Standards II*, 1993, Academic Press, San Diego, CA (1993).

[13] M. Herman, *Mol. Phys.* **105**, 2217 (2007).

Figure captions

Figure 1: A portion of the infrared spectrum of $^{13}CH^{12}CH$ showing the Q-branches of the $2\nu_3+\nu_5(\Pi) \leftarrow GS(\Sigma^+)$ and $2\nu_2+2\nu_4+3\nu_5(\Pi) \leftarrow GS(\Sigma^+)$ band. Experimental conditions: pressure 0.505 kPa, optical path length 55.1 m.

Figure 2: A portion of the infrared spectrum of $^{13}CH^{12}CH$. Three main bands are highlighted: $\nu_1+2\nu_2+\nu_5(\Pi) \leftarrow GS(\Sigma^+)$, $3\nu_2+3\nu_5(\Pi) \leftarrow GS(\Sigma^+)$ and $2\nu_1+\nu_4+\nu_5(\Sigma^+) \leftarrow GS(\Sigma^+)$. Experimental conditions: pressure 4.84 kPa, optical path length 55.1 m.

Figure 3: A portion of the infrared spectrum of $^{13}CH^{12}CH$ showing the Q-branches of the following bands: $2\nu_1+2\nu_5(\Sigma^+) \leftarrow \nu_5(\Pi)$, $2\nu_1+\nu_4+\nu_5(\Sigma^+) \leftarrow \nu_4(\Pi)$, $2\nu_1+\nu_4+\nu_5(\Sigma^-) \leftarrow \nu_4(\Pi)$, $2\nu_1+2\nu_5(\Delta) \leftarrow \nu_5(\Pi)$, $2\nu_1+ \nu_4+\nu_5(\Delta) \leftarrow \nu_4(\Pi)$. The stronger lines are from the P branch of the $2\nu_1+\nu_5(\Pi) \leftarrow GS(\Sigma^+)$ band. Experimental conditions: pressure 4.84 kPa, optical path length 55.1 m.

Figure 4: A portion of the infrared spectrum of $^{13}CH^{12}CH$ showing the Q-branch of the $2\nu_1+\nu_4(\Pi) \leftarrow GS(\Sigma^+)$ band. The stronger lines are from the R branches of the $\nu_1+\nu_3+\nu_5(\Pi) \leftarrow GS(\Sigma^+)$ and $\nu_2+\nu_3+\nu_4+2\nu_5(\Pi) \leftarrow GS(\Sigma^+)$, bands. Experimental conditions: pressure 4.84 kPa, optical path length 55.1 m.

Table captions

Table 1: Band centers (ν_c), vibrational term values (G_v) and rotational constants (in cm^{-1}) in $^{13}CH^{12}CH$. The standard deviation (1σ) is indicated in parentheses in the unit of the last quoted digit. The assigned lines are mentioned for each branch. The last column gives the number and standard deviation of the lines included in the fit. Rotational lower state constants were constrained during the analysis, from [3].

Table 1

$v_1 v_2 v_3 v_4 v_5$, l_4 l_5	Transition	ν_c	G_v	B_v	D_v x 10^6	H_v x 10^9	q_v x 10^3 q_J x 10^6 q_{JJ} x 10^9	P,Q,R {J_{min},J_{max}}	n. of lines σ_{lines} x 10^3
0 0 2 1 0, 1 0	$\Pi - \Pi$ (ν_5)	6350.70734(13)	7080.0739	1.1387039(15)	1.5916(41)	0.0481(32)	5.72476(78) –0.0268(12)	P_e{2,32} ; R_e{1,26} P_f{2,32} ; R_f{1,26}	87 0.47
0 1 1 3 0, 1 0	$\Pi - \Pi$ (ν_4)	6392.43111(52)	7000.7755	1.140454(15)	–4.30(11)	–1.27(21)	10.413(16) –2.44(15) –5.41(35)	P_e{3,22} ; R_e{1,16} P_f{3,25} ; R_f{1,15}	55 1.32
0 0 2 1 0, 1 0	$\Pi - \Pi$ (ν_4)	6471.73128(15)	7080.0739	1.1387052(16)	1.5934(40)	0.0484(26)	5.72604(98) –0.0277(12)	P_e{2,36} ; R_e{1,30} P_f{2,34} ; R_f{1,29}	99 0.69
0 0 2 0 1, 0 1	$\Pi - \Pi$ (ν_5)	6475.59154(26)	7204.9599	1.1404349(46)	2.939(19)	0.787(21)	4.6238(54) 0.604(28) –0.624(34)	P_e{2,26} ; R_e{1,23} P_f{2,27} ; R_f{1,20}	68 0.89
1 0 1 1 0, 1 0	$\Pi - \Pi$ (ν_4)	6517.16692(14)	7125.5087	1.1378970(39)	1.934(29)	3.013(54)	5.4521(54) 0.549(52) –4.42(10)	P_e{2,17} ; R_e{1,21} P_f{2,20} ; R_f{1,29}	62 0.45
1 0 1 0 1, 0 1	$\Pi - \Pi$ (ν_5)	6520.05662(16)	7249.4229	1.1384201(23)	1.7193(81)	0.2213(81)	4.8885(29) –0.070(13) –0.363(15)	P_e{2,29} ; R_e{1,26} P_f{2,31} ; R_f{1,29}	94 0.63
2 0 0 1 0, 1 0	$\Pi - \Pi$ (ν_5)	6543.07663(14)	7272.4416	1.1370759(25)	1.501(10)	–0.084(11)	4.8745(13) –0.0348(31)	P_e{2,25} ; R_e{1,23} P_f{2,24} ; R_f{1,24}	58 0.41
0 2 0 1 3, 1 -1	Σ^+ – G.S.	6589.76247(41)	6589.7625	1.1423606(92)	5.351(44)	1.434(46)		P{1,30} ; R{0,28}	33 1.07

0 0 2 0 1, 0 1	$\Pi - \Pi\ (\nu_4)$	6596.61590(25)	7204.9602	1.1404218(36)	2.856(12)	0.670(10)	4.6226(42) 0.568(18) –0.533(17)	P_e{2,27} ; R_e{1,30} P_f{2,27} ; R_f{1,29}	74 0.89
0 1 1 1 2, 1 0	$\Pi - \Pi\ (\nu_4)$	6621.84935(52)	7230.1951	1.1418843(96)	2.216(35)		9.0096(35)	P_e{2,17} ; R_e{1,16} P_f{2,17} ; R_f{3,19}	40 1.51
2 0 0 1 0, 1 0	$\Pi - \Pi\ (\nu_4)$	6664.10007(11)	7272.4411	1.13708662(76)	1.56053(94)		4.86832(91) –0.0224(14)	P_e{2,25} ; R_e{1,28} P_f{2,24} ; R_f{1,30}	77 0.47
2 0 0 0 1, 0 1	$\Pi - \Pi\ (\nu_5)$	6664.79196(11)	7394.1578	1.13792029(91)	1.66094(12)		4.8371(11) –0.1065(19)	P_e{2,18} ; R_e{2,28} P_f{2,22} ; R_f{1,26}	70 0.50
0 1 1 3 0, 1 0	Π – G.S.	6999.63641(43)	7000.7768	1.140375(15)	–5.14(13)	–3.48(30)	10.450(19) –2.82(20) –4.35(53)	P{3,23} ; R{0,18} Q{1,16}	42 1.06
0 3 0 1 1, 1 -1	Σ^+ – G.S.	7063.48837(25)	7063.4884	1.1335475(24)	3.0484(42)			P{1,26} ; R{0,23}	36 0.78
0 0 2 2 0, 0 0	$\Sigma^+ - \Pi\ (\nu_4)$	7067.40254(52)	7674.6064	1.140295(19)	–15.89(16)	–18.13(29)		P{2,18} ; R{2,15} Q{2,22}	23 0.91
0 0 2 1 0, 1 0	Π – G.S.	7078.93548(11)	7080.0742	1.1386998(12)	1.5759(31)	0.0352(20)	5.7328(16) –0.0595(50) –0.0265(35)	P{2,35} ; R{0,28} Q{1,32}	72 0.42
1 0 1 1 1, 1 -1	$\Sigma^+ - \Pi\ (\nu_5)$	7088.68130(32)	7816.9092	1.1407093(40)	4.7635(91)			P{1,18} ; R{1,21} Q{1,18}	40 1.06
1 0 1 1 1, 1 1	$\Delta - \Pi\ (\nu_5)$	7100.90300(25)	7833.6904	1.1398781(31)	0.6080(75)		–0.0021645(33)	P_e{4,20} ; R_e{2,19} P_f{4,19} ; R_f{2,17} Q_f{3,21} ; Q_e{3,21}	73 0.93

1 0 1 2 0, 2 0	$\Delta - \Pi$ (ν_4)	7104.46131(32)	7716.2130	1.1369406(44)	2.290(17)	0.615(19)	4.6191(61) 0.955(30) –1.157(36)	P_e{3,25} ; R_e{1,21} P_f{3,29} ; R_f{1,25} Q_e{2,25}	72 0.86
1 0 1 2 0, 0 0	$\Sigma^+ - \Pi$ (ν_4)	7104.48566(64)	7711.6896	1.1451797(99)	2.298(39)	0.174(40)		Q{3,25}	18 0.87
0 1 1 2 1, 2 -1	Π – G.S.	7105.87479(24)	7107.0158	1.1410373(36)	2.8724(81)		5.8891(45) 0.108(12)	P{2,23} ; R{0,20} Q{1,23}	45 0.78
0 2 1 1 0, 1 0	$\Pi - \Pi$ (ν_4)	7110.93467(17)	7719.2706	1.1320481(12)	1.5637(14)		5.1725(14) –0.0278(21)	P_e{2,31} ; R_e{1,26} P_f{2,30} ; R_f{1,26}	87 0.79
1 0 1 1 0, 1 0	Π – G.S.	7124.36832(69)	7125.5063	1.138010(13)	2.531(41)	1.610(34)	5.455(16) 0.209(62) 0.849(55)	P{2,38} ; R{0,30} Q{1,29}	54 2.42
0 2 1 0 0, 0 0	Σ^+ – G.S.	7145.380357(74)	7145.3804	1.13099659(38)	1.53906(35)			P{1,37} ; R{0,35}	64 0.31
1 1 0 2 1, 2 -1	Π – G.S.	7165.23314(39)	7166.3754	1.1422350(69)	4.188(29)	0.170(33)	3.8178(58) 0.955(17)	P{3,21} ; R{0,20} Q{1,26}	46 1.10
0 0 2 0 2, 0 0	$\Sigma^+ - \Pi$ (ν_5)	7177.95110(28)	7906.1790	1.1419801(36)	4.0850(95)			P{1,21} ; R{5,17} Q{1,17}	35 0.75
1 1 0 2 1, 0 1	Π – G.S.	7181.20779(36)	7182.3490	1.1412183(34)	0.9568(62)		–3.4167(51) –0.775(11)	P{2,25} ; R{0,26} Q{1,24}	38 1.11
0 0 2 1 1, 1 -1	$\Sigma^- - \Pi$ (ν_4)	7182.94690(25)	7790.1508	1.1408154(22)	1.6739(37)			P{3,26} ; R{2,24} Q{2,25}	53 0.84
0 0 2 0 2, 0 2	$\Delta - \Pi$ (ν_5)	7187.63931(27)	7920.4332	1.1414904(46)	0.478(20)	–0.205(22)	–0.0024470(84) 0.000377(16)	P_e{3,25} ; R_e{1,22} P_f{3,24} ; R_f{1,23} Q_f{2,25} ; Q_e{2,25}	98 1.01

0 0 2 0 1, 0 1	Π – G.S.	7203.81986(29)	7204.9603	1.1404021(40)	2.703(10)	0.4843(67)	4.6297(50) 0.386(15) –0.275(10)	P{2,30} ; R{0,35} Q{1,38}	58 1.01
0 2 0 2 3, 0 1	Π – G.S.	7205.66668(27)	7206.8096	1.1427753(61)	0.111(31)	–0.808(40)	3.2870(81) –0.860(49) 0.890(69)	P{2,21} ; R{0,23} Q{2,22}	55 0.88
0 1 1 1 2, 1 0	Π – G.S.	7229.05408(22)	7230.1959	1.1418423(33)	1.8768(86)	–0.2706(63)	8.9257(48) 0.801(14) –0.822(11)	P{2,31} ; R{0,31} Q{1,30}	62 0.71
1 0 1 0 1, 0 1	Π – G.S.	7248.28396(12)	7249.4224	1.1384222(15)	1.7255(47)	0.2277(41)	4.8867(18) –0.0635(74) –0.3685(72)	P{2,28} ; R{0,28} Q{1,32}	71 0.41
2 0 0 1 0, 1 0	Π – G.S.	7271.30393(24)	7272.4410	1.1370905(21)	1.5666(33)		4.8612(12)	P{3,20} ; R{2,20} Q{1,28}	52 0.95
1 1 0 1 2, 1 0	Π – G.S.	7278.47865(76)	7279.6164	1.137777(10)	2.710(28)			P{5,19} ; R{0,18}	25 1.57
2 0 0 0 2, 0 0	$\Sigma^+ - \Pi$ (ν_5)	7361.58669(27)	8089.8146	1.1405489(35)	4.484(11)	0.6650(96)		P{1,29} ; R{1,25} Q{1,22}	57 0.71
2 0 0 1 1, 1 -1	$\Sigma^+ - \Pi$ (ν_4)	7362.66167(19)	7969.8656	1.1395671(29)	3.319(10)	0.1381(97)		P{3,28} ; R{2,28} Q{1,23}	58 0.60
2 0 0 1 1, 1 -1	$\Sigma^- - \Pi$ (ν_4)	7367.02549(18)	7974.2294	1.1391357(13)	1.6095(18)			P{1,30} ; R{1,27} Q{1,25}	68 0.75
2 0 0 0 2, 0 2	$\Delta - \Pi$ (ν_5)	7371.29700(22)	8104.0846	1.1399314(36)	0.375(12)		–0.002495(22) 0.000298(78)	P_e{3,20} ; R_e{1,21} P_f{3,18} ; R_f{1,16} Q_f{2,19} ; Q_e{2,17}	87 0.88

2 0 0 1 1, 1 1	$\Delta - \Pi$ (ν_4)	7375.78926(22)	7987.5492	1.1390011(22)	0.7746(45)		–0.003497(17) 0.000166(40)	P_e{7,24} ; R_e{2,18} P_f{7,25} ; R_f{4,21} Q_f{2,22} ; Q_e{2,23}	87 0.80
2 0 0 0 1, 0 1	Π – G.S.	7393.018981(85)	7394.1569	1.13793005(66)	1.6350(11)	0.01825(51)	4.84799(86) –0.1377(18) –0.02035(86)	P{2,39} ; R{0,39} Q{1,40}	111 0.40
1 1 0 0 3, 0 1	Π – G.S.	7419.50638(19)	7420.6495	1.1431668(21)	2.8756(53)	0.0384(36)	10.1759(31) –0.4045(94) –0.3890(66)	P{2,31} ; R{0,31} Q{15,32}	71 0.65
0 2 0 0 5, 0 1	Π – G.S.	7445.10236(45)	7446.2478	1.145413(11)	2.999(65)	–1.332(94)	12.600(14) –0.734(97) 0.75(16)	P{3,17} ; R{0,25} Q{4,20}	40 1.15
0 0 2 2 0, 0 0	Σ^+ – G.S.	7674.60373(71)	7674.6037	1.140349(24)	–15.83(20)	–19.53(43)		P{1,22} ; R{0,21}	31 1.49
1 0 1 3 0, 1 0	$\Pi - \Pi$ (ν_4)	7695.61639(46)	8303.9630	1.142750(17)	9.77(16)	–6.03(42)	11.648(19) –3.92(24) –26.36(72)	P_e{2,15} ; R_e{1,17} P_f{2,16} ; R_f{1,14}	42 1.09
0 1 1 3 1, 1 -1	Σ^+ – G.S.	7704.18800(55)	7704.1880	1.1420142(98)	–3.703(40)	–3.822(43)		P{1,28} ; R{0,26}	39 1.62
1 0 1 2 0, 2 0	Δ_e – G.S.	7711.68931(33)	7716.2270	1.1344294(54)	2.301(21)	0.900(23)		P{3,27} ; R{2,24}	44 0.81
1 0 1 2 0, 0 0	Σ^+ – G.S.	7711.69171(33)	7711.6917	1.1451451(34)	2.1656(82)	0.0350(54)		P{1,32} ; R{0,31}	52 0.86
0 2 0 3 3, 1 -1	Σ^+ – G.S.	7725.56610(30)	7725.5661	1.1456798(77)	11.707(46)	3.126(71)		P{1,20} ; R{0,20}	31 0.77

1 1 0 3 1, 3 -1	Δ_e – G.S.	7754.46091(94)	7759.0096	1.137175(18)	4.049(85)	1.63(11)		P{5,20} ; R{3,21}	31 1.54
1 1 0 3 1, 1 -1	Σ^+ – G.S.	7754.48122(95)	7754.4812	1.148409(26)	1.67(17)	–2.36(29)		P{2,20} ; R{2,19}	28 1.67
1 2 0 0 1, 0 1	Π – G.S.	7921.40797(24)	7922.5411	1.1331639(32)	2.1042(94)	0.2240(74)	5.8010(19) –0.4199(29)	P{2,29} ; R{0,29} Q{1,30}	76 0.94
0 3 0 0 3, 0 1	Π – G.S.	7939.42582(42)	7940.5608	1.1349954(88)	1.965(42)	–0.519(57)	7.7901(71) 0.112(22)	P{2,23} ; R{0,20} Q{1,24}	57 1.40
2 0 0 1 1, 1 -1	Σ^+ – G.S.	7969.86102(45)	7969.8610	1.1396139(56)	3.330(12)			P{1,22} ; R{0,21}	33 1.38
0 2 1 1 1, 1 -1	Σ^+ – G.S.	8414.81985(34)	8414.8199	1.1329761(59)	2.364(23)	0.241(23)		P{1,27} ; R{0,24}	42 1.01
1 0 1 2 1, 2 -1	Π – G.S.	8420.0184(14)	8421.1484	1.129992(30)	–1.42(17)	–3.78(28)		P{4,21} ; R{2,13}	22 1.91
0 3 0 2 3, 2 -1	$\Pi - \Pi$ (ν_4)	8422.43632(32)	9030.7763	1.1360591(63)	3.484(30)	–0.354(38)	10.5601(77) –2.789(45) 0.498(62)	P_e{2,20}; R_e{1,22} P_f{2,24}; R_f{2,18}	67 1.04
1 1 1 1 0, 1 0	$\Pi - \Pi$ (ν_4)	8432.67452(47)	9041.0135	1.1350476(76)	1.306(29)	–0.996(29)	8.8202(75) 1.689(29)	P_e{2,25}; R_e{1,20} P_f{3,27}; R_f{2,25}	65 1.43
0 1 2 0 0, 0 0	Σ^+ – G.S.	8435.21910(25)	8435.2191	1.1324443(62)	6.276(34)	3.458(51)		P{1,26} ; R{0,25}	37 0.66
2 1 0 1 0, 1 0	$\Pi - \Pi$ (ν_5)	8456.88934(32)	9186.2497	1.1324484(61)	1.329(28)	0.220(36)	4.9879(71) 1.231(42) 0.264(60)	P_e{2,21}; R_e{2,24} P_f{2,22}; R_f{1,21}	68 0.99

1 1 1 0 0, 0 0	Σ^+ – G.S.	8464.22734(21)	8464.2273	1.1324153(24)	2.7898(66)	0.3530(47)		P{1,35} ; R{0,35}	58 0.69
0 3 0 1 3, 1 -1	Σ^+ – G.S.	8475.68592(14)	8475.6859	1.1348687(15)	5.7283(39)	1.2685(27)		P{1,33} ; R{0,30}	55 0.46
1 2 0 1 1, 1 -1	Σ^+ – G.S.	8491.44260(18)	8491.4426	1.1342984(36)	4.786(16)	0.990(19)		P{1,25} ; R{0,24}	40 0.54
2 1 0 0 0, 0 0	Σ^+ – G.S.	8607.80135(43)	8607.8014	1.1303157(40)	1.7197(71)			P{2,18} ; R{2,23}	31 1.13
0 3 0 2 3, 2 -1	Π – G.S.	9029.6732(13)	9030.8096	1.136440(26)	3.16(16)	–1.21(27)	12.236(26) –6.12(22) 4.25(45)	P{7,17} ; R{5,17} Q{1,21}	32 1.85
1 1 1 1 0, 1 0	Π – G.S.	9039.87611(26)	9041.0113	1.1351474(30)	1.9267(62)		8.8711(39) 1.521(10)	P{2,23} ; R{0,18} Q{1,23}	53 0.98
0 3 1 0 0, 0 0	Σ^+ – G.S.	9054.18740(68)	9054.1874	1.1249112(81)	1.335(25)	–0.153(20)		P{1,29} ; R{0,28}	38 1.70
2 1 0 0 1, 0 1	Π – G.S.	9311.36544(32)	9312.4984	1.1329599(49)	2.136(17)	0.209(15)	5.8435(61) –0.632(26) 0.165(25)	P{3,23} ; R{0,26} Q{1,29}	60 1.10
0 3 0 0 5, 0 1	Π – G.S.	9328.54154(79)	9329.6784	1.136851(91)	3.018(22)		9.079(10) 0.835(34)	P{8,18} ; R{4,17} Q{1,21}	26 1.48

[a] The values of ρ_v and ρ_v^J defined in equation (2) are listed for Δ states, instead of those of q_v and q_v^J. The standard deviation (1σ) is indicated in parentheses in the unit of the last quoted digit. The assigned lines are listed for each branch. The last column gives the number of lines included in the fit and the corresponding standard deviation.

[b] constrained in the fitting procedure to the values from [3] or to zero.